EXPERIMENTAL INVESTIGATION OF FLOW AND HEAT TRANSFER CHARACTERISTICS ON MATRIX RIBBED CHANNEL

by

Bo ZHANG[a*], Quan HONG[a], Yuanyuan DOU[a], Honghu JI[a], and Rui CHEN[b]

[a] Jiangsu Province Key Laboratory of Aerospace Power System, College of Energy and Power, Nanjing University of Aeronautics and Astronautics, Nanjing, China
[b] Aeronautical and Automotive Engineering, Loughborough University, Leicester, UK

Original scientific paper
https://doi.org/10.2298/TSCI190702026Z

The effect of the rib width to height ratio t/e and width to pitch ratio t/p on the local heat transfer distribution in a rectangular matrix ribbed channel with two opposite in line 45° ribs are experimentally investigated for Reynolds numbers from 54000 to 150000. The rib height to channel height ratio e/H is 0.5, t/p and t/e both varies in range of 0.3-0.5. To simulate the actually situation in turbine blades, and provide useful direct results for turbine blade designers, the parameters are same with the blade. The experiments results show that, in comparison to fully developed flow in a smooth pipe of equivalent hydraulic diameter, the Nusselt number inside the matrix-ribbed rectangular channel is increased up to 5 to 9 times higher, while total pressure drop is enlarged by up to significant magnitude. The Nusselt number ratio increases with t/p and t/e increased. Semi-empirical heat transfer is developed for designing of cooling channel.

Key words: *matrix ribbed channel, heat transfer enhancement, blade cooling, aero engine*

Introduction

To increase the efficiency of a gas turbine, the common approach is to increase the turbine inlet temperature. In order to allow the gas turbine designers to increase the turbine inlet temperature while maintaining an acceptable temperature for the structures, advanced cooling methods are developed.

Different cooling schemes must be used in different regions of the air-foil depending on the thermal load and mechanical strength requirements. Leading edge is generally cooled by jet impingement, the trailing edge is cooled by pin fins, while serpentine passages with rib turbulators are usually applied to cool the middle portion of the gas turbine air-foils [1-3].

Internal cooling passages are made in some of the turbine blades during its manufacturing and hence to allow high inlet temperatures to achieve high thrust/weight ratios and low specific fuel consumption. As a kind of Internal cooling methods, ribbed passages are widely used in internal cooling of turbine blades middle portion, which are commonly used to create a secondary flow, disturb the wall sub layer, increase flow turbulence, and create separation and reattachment, which result in a higher heat transfer coefficient.

* Corresponding author, e-mail: zhangbo_pe@nuaa.edu.cn

Studies on ribs have paid attention to many configuration parameters of ribbed channels, such as rib shape, aspect ratio, pitch ratio, *p*/*e*, blockage ratio, *e*/*Dh*, rib angle of attack, *a*, inclination of ribs, rotation of ribs and arrangement (staggered or parallel) [4-8].

Alfarawi [9] experimentally investigated heat transfer enhancement from rectangular duct roughened by hybrid ribs, obtained the effect of *P*/*e*, and obtained correlations for Nu/Nu_s, f/f_s, and $(Nu/Nu_s)/(f/f_s)$ 1/3*. Liou *et al.* [10] investigated the heat transfer enhancement of periodical ribbed channel.

Bailey *et al.* [11] experimentally investigated heat transfer and flow characteristics in a high blockage channel whose e/H was from 0.275 to 0.475, Chanteloup [12] measured 3-D flow and heat transfer coefficiency in a two-pass 45º crossed ribbed channel, Viswanathan [13] numerical investigated flow and heat transfer characteristics in an internal high blockage ratio ribbed channel, and made a comparison with that of Carcasci [14] and Baily *et al.* [11].

Large *e*/*Dh* can not only bring high heat transfer characteristics, but significant friction accompanied [15-17]. To raise the heat transfer to some great extent, we can increase the *e*/*De* as large as it can be. As the height of crossed ribs was increased to half of the channel height, the ribs on top and bottom walls connected, and no free flow space left. An interesting creatively cooling technique is constructed, named matrix cooling channel [13], which was first seen in the early Soviet design in 1970s [18].

In many researches, the axial length of ribbed channel was designed long enough to obtain the fully hydrodynamically developed period, however, in a true turbine blade, the axial length was so short to fit the limited space, and minimize the weight, which made the fluid cannot reach the fully developed period, and leads much difference in the flow and heat transfer characteristics.

In this paper, matrix-ribbed channels with different geometrical parameters are designed, the geometrical parameters were designed according to the actually situation in blade, and the flow situations were similar with the turbine blades, in which the heat transfer and friction characteristics were experimentally investigated.

Experimental system

Figure 1 showed schematically the layout of an experimental apparatus. Rib geometry details were shown in tab. 1. The forced air went through a compressor with high pressure of 8 atm (1 atm = 101325 Pa), and then passed through a setting chamber and a diameter orifice

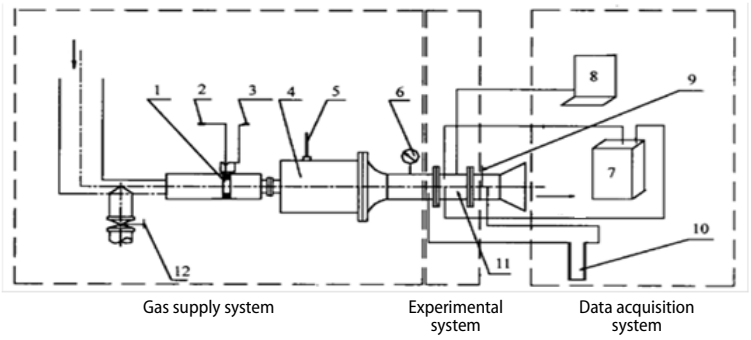

Figure 1. Sketch of experimental system; *1 – orifice meter, 2 – pressure sensor, 3 – pressure sensor 4 – plenum chamber, 5 – thermometer, 6 – pressure gauge, 7 – heater, 8 – computer, 9 – pressure gauge, 10 – water drainage, 11 – experimental duct, 12 – valve*

* s – smooth tube

plate to measure the flow rate. A metal plenum was set between the pipe and the test channel which used to ensure the air entered the test channel under full developed condition, at the end of the channel, the air flew out. The Reynolds number computed from the channel hydraulic diameter, (100 × 80 mm^2 cross-section) D, was varied between $5.4 \cdot 10^4$-$1.5 \cdot 10^5$, which was the actually region in turbine blades.

The inlet and outlet pressure were measured by two Pitot, and the inlet gas temperature was measured by three *K*-style thermal couples at the entrance.

Experimental models

A schematic drawing showed the ribbed wall configuration in fig. 2.

The wall length was 76.4 mm, the ribbed length was 68.4 mm, the width was 192 mm, with 8 mm smooth channels both at the top and bottom sides, all ribs had an angle with the flow at 45°, the ribs distance was marked as P, and rib width marked as t, the two parameters were changeable in the paper. All ribs have same height of 7.6 mm, with a 2 mm thick wall, and the thermal couples were place along the center line.

Figure 3 shown the sketches of matrix ribbed channel composed by two same ribbed plates with 45° line ribs shown in fig. 2. As could be seen, the ribs were staggered on two opposite walls, the rib height grew to half of the channel, leaving no free space between up and down opposite ribs.

Figure 4 showed the completed matrix ribbed channel, to see clearly, the local cutaway view was given out. The upper and lower horizontal walls of the test section made of aluminum plate were heat transfer surfaces, and the two vertical walls (Bakelite plates) connecting the two ribbed walls were thermally insulated. Two flange plates used in the entrance and exit of ribbed channel were both made of 5 mm thick Bakelite to minimize the axial heat loss.

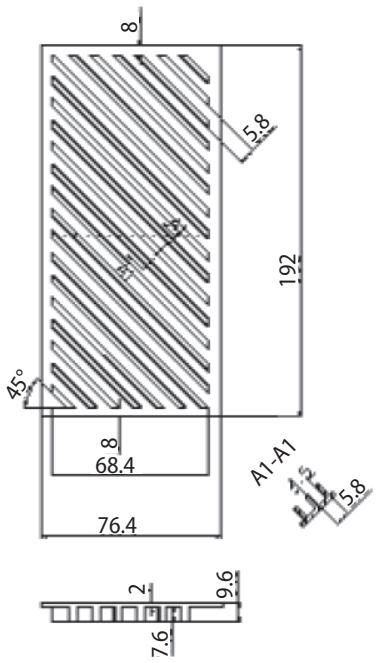

Figure 2. Schematic drawing

The ribbed walls were made of 3 mm thick aluminum plate, heated by the 0.15 mm thick constantan heating foil posted on both upper and lower surface. The aluminum plates were highly polished to minimize emissivity, as shown in fig. 5. The heat loss outside the test duct was under 5% of the total heat flux.

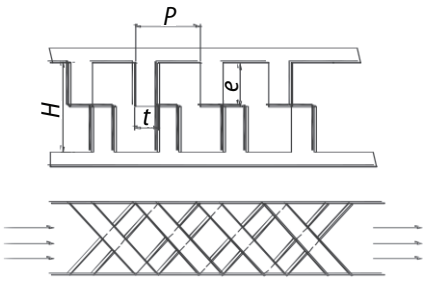

Figure 3. Different perspectives of schematic of matrix ribs

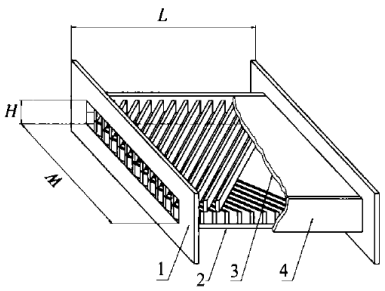

Figure 4. Part sectional view of ribbed channel

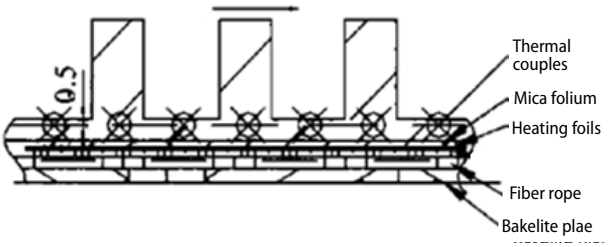

Figure 5. Sketch of insulation and heat preservation

Table 1. Geometrical parameter

α [°]	t [mm]	e [mm]	p [mm]	t/e	t/p
45	1.9	7.6	5.7	0.25	0.33
45	2.3	7.6	9.12	0.30	0.33
45	3.8	7.6	11.4	0.50	0.33
45	2.3	7.6	9.12	0.30	0.25
45	2.3	7.6	4.56	0.30	0.50

So the heat flux could be calculated as $q = UI$ (in which, the U represents the voltage between the heating film and I represents the current through the film, the U, I were measured by voltmeter and ammeter, separately)

Heat transfer measurements were performed for an area between a pair of ribs and under every rib.

The geometrical parameters were listed in tab. 1. There were five models in all, each of them consists of two same plates listed in tab. 1. (For example, Model 1 consisted of two plate 1, shared the same a = 45°, and rib height e = 7.6 mm, which was half of the channel height.)

Model 1, 2, 3 had the same t/p value and different t/e values, focused on the effect of t/e, while Model 2, 4, 5 focused on effect of t/p. The heat transfer and friction characteristics of matrix channels composed of the two same listed ribbed plates were experimentally studied in the paper.

The local heat transfer coefficient was calculated from the local net heat transfer rate per unit surface area to the cooling air, the local wall temperature on each allium plate, and the local bulk mean air temperature:

$$h = \frac{q - q_{\text{loss}}}{A(T_w - T_f)} \tag{1}$$

The local net heat transfer rate was the electrical power generated from the foil heaters (calculated as $q = U^2/R$, where U was the voltage on each side of the test duct, and R was measured foil resistance) minus the heat loss outside the test duct.

Some of the main parameters were defined:

– The local Nusselt number was defined:

$$\text{Nu}_x = \frac{hx}{\lambda} \tag{2}$$

$$h_x = \frac{q}{T_{wi} - T_{fx}} \tag{3}$$

The T_{wx} were measured by thermocouples, and T_{fx} was computed:

$$T_{fx} = T_{f1} - \frac{(T_{f1} - T_{f2})x}{L} \tag{4}$$

The T_{f1} and T_{f2} were the flow temperatures measured by thermocouples at the entrance and exit planes, x was the local distance, and L was whole plate length.

Surface averaged Nusselt number was defined:

$$\mathrm{Nu} = \frac{h\mathrm{De}}{\lambda} \tag{5}$$

$$h = \frac{q}{\overline{T}_w - T_f} \tag{6}$$

$$\mathrm{De} = \sqrt{\frac{4A}{\pi}} \tag{7}$$

$$\mathrm{Re} = \frac{\rho u d}{\lambda} \tag{8}$$

where u was the velocity of entrance without ribs, $d = (4A/\pi)^{1/2}$ was the equivalent diameter, A was the entrance area of the ribbed channel, μ was the air dynamic viscosity.

$$T_f = \frac{T_{f1} + T_{f2}}{2}, \quad \overline{T_w} = \frac{1}{N}\sum_i^N T_{wi} \tag{9}$$

The local Nusselt number of the present study was normalized by the Nusselt number for fully developed turbulent flow in smooth circular tubes, correlated by Dittus-Boelter/ McAdams as:

$$\frac{\mathrm{Nu}}{\mathrm{Nu}_{FD}} = \frac{\dfrac{hl}{\lambda}}{0.023\,\mathrm{Re}^{0.8}\,\mathrm{Pr}^{0.4}} \tag{11}$$

where Nu_{FD} was Nusselt number for the fully developed turbulent flow in smooth circular tube.

Experimental results and discussion

About the Nusselt number distribution along axial direction, large fluctuations were shown, which might be induced by the influence of thermal entrance, for the channel's length did not achieve hydrodynamically developed state. However, the results were the specific results inside the small turbine blade.

In the paper, non-dimensional parameters Reynolds number and t/e, t/p, were taken into account. The semi correlation of the average Nusselt number with t/p and Reynolds number could be written:

$$\mathrm{Nu} = 90.92\left(\frac{t}{p}\right)^{1.185}\mathrm{Re}^{0.365} \tag{12}$$

where t/p was varied between 0.3 and 0.5, as t/e = 0.33. Reynolds number varied between $0.5\cdot10^4 \le \mathrm{Re} \le 1.5\cdot10^5$, Reynolds number was the value of entrance without ribs, which was the same in hereafter this paper.

Figure 6 further showed the comparison of the curves computed from the eq. (12) with the experimental data *vs.* Reynolds number. The Nusselt number increased with Reynolds number increased, and with the increasing of t/p, the Nusselt number increased gradually. It was satisfied for the matrix ribbed geometry, the curves fitted the experimental data well, with the data distributed on both sides. For the correlation was the comprehensive result of different t/p

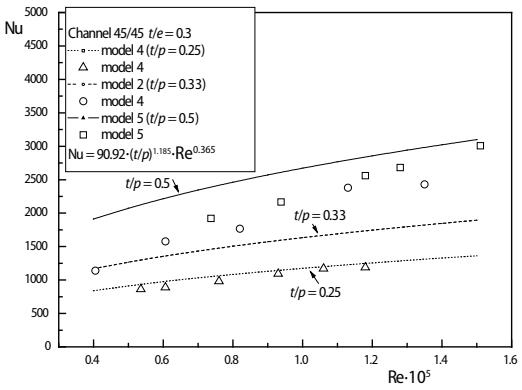

Figure 6. Nusselt number distributions in different *t*/*p* models

models, so the curves did not fit each data to the same degree, but satisfied the fundamental requirements of all data.

The correlation of the average Nusselt number with *t*/*e* and Reynolds number can be written:

$$\mathrm{Nu} = 3.065\left(\frac{t}{e}\right)^{-0.42} \mathrm{Re}^{0494} \qquad (13)$$

where *t*/*e* was varied between 0.3 and 0.5, as $t/p = 0.33$.

Figure 7 showed the comparison of the computed curves with the experimental data from the eq. (13). The correlation satisfied the fundamental requirements of all data.

To show the heat transfer augmentation of matrix ribbed channel against the smooth ones, Nusselt number ratio $\mathrm{Nu}/\mathrm{Nu}_{FD}$ were defined, and the results of different *t*/*p* and different *t*/*e* were all illustrated in figs. 8 and 9.

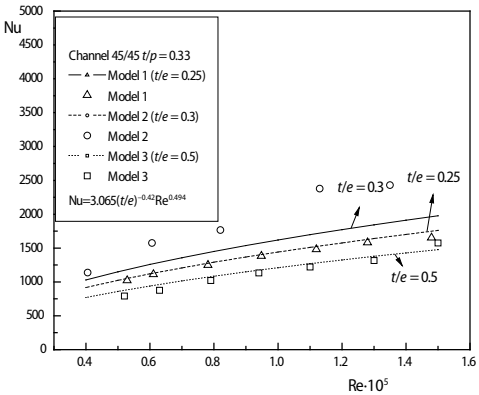

Figure 7. Nusselt number distributions for different in *t*/*e* models

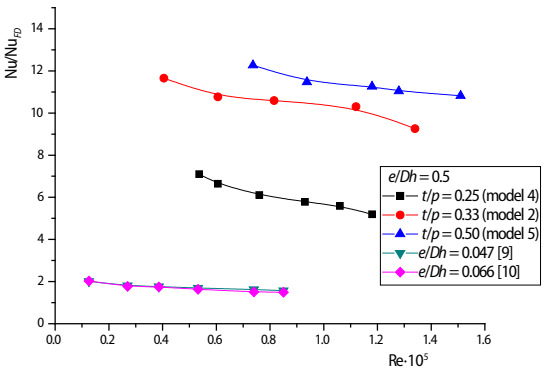

Figure 8. The $\mathrm{Nu}/\mathrm{Nu}_{FD}$ distributions for different *t*/*p* models

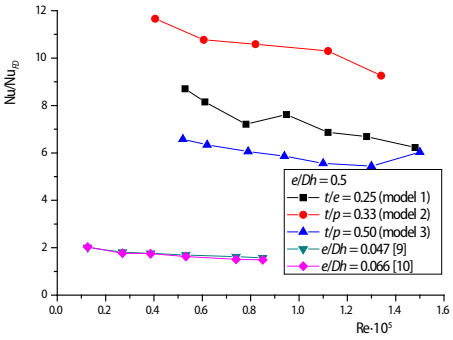

Figure 9. The $\mathrm{Nu}/\mathrm{Nu}_{FD}$ distributions for different *t*/*e* models

Figure 8 presented the distribution of $\mathrm{Nu}/\mathrm{Nu}_{(FD)}$ in Models with different *t*/*p* *vs.* Reynolds number, and the data of normal ribbed models in [9, 10] were given too. The $\mathrm{Nu}/\mathrm{Nu}_{(FD)}$ all decreased as Reynolds number increased, the $\mathrm{Nu}/\mathrm{Nu}_{(FD)}$ could achieve above 13 as $t/p = 0.5$ in matrix ribbed channel in this paper, while those of normal ribbed channel only reached lower than 2.5. The results indicated that Nusselt number of the matrix ribbed wall was about 5 times higher than normal ribbed one, and more than ten times larger than the smooth wall, due to the influence

of high block ratio. The heat transfer coefficient of the ribbed channel is much larger than the thermal conductivity of the stainless steel.

Figure 9 presented the distribution of $Nu/Nu_{(FD)}$ in Models with different t/e *vs.* Reynolds number, and the data of normal ribbed models in [9, 10] were given too. The $Nu/Nu_{(FD)}$ all decreased as Reynolds number increased, the $Nu/Nu_{(FD)}$ could achieve above 12 as $t/e = 0.33$ in matrix ribbed channel in this paper, while those of normal ribbed channel only reached lower than 2.5.The results also indicated that the matrix ribbed channel induced a wonderful enhancement in heat transfer as showed in fig. 9.

As mentioned in [12], the rib induced secondary flow, and changing of t/p and t/e may change the secondary flow shape and magnitude of cells. Further, as shown in figs. 8 and 9, Nusselt number of the matrix ribbed channel was 4-7 times higher than those of normal ribbed channel in [9, 10], result in much higher heat transfer characteristics.

The semi correlations for staggered rib alignments with the parameters ranges, $0.3 \le t/e \le 0.5$, $0.3 \le t/p \le 0.5$, $0.5 \cdot 10^4$-$1.5 \cdot 10^5$, $\alpha = 45^o$.

Conclusions

The combined effects of rib t/e and t/p values on heat transfer and friction factor for flow in rectangular ducts with opposite matrix ribbed walls were experimentally investigated for Reynolds numbers ranging from 50000 to 150000. The following conclusions were drawn.

- Matrix ribbed channels raised heat transfer characteristics, the Nusselt number ratio grown to 14 times of that of smooth one, and decreased with Reynolds number increased. The Nusselt number increased with increase of t/p monotonously, $t/p = 0.5$ obtained the maximum value. While with t/e increased, the Nusselt number shown a non-monotonously changing, increased first then decreased, $t/e = 0.33$ obtained the maximum value.
- In the matrix ribbed channel, fluid was forced to move up and down between adjacent ribs, the winding passage enhanced the convective heat transfer between fluid and wall, leads to a wonderful heat transfer characteristic.
- The semi-empirical correlation of the Nusselt number are developed based on all matrix rib configurations with different t/p and t/e values, to account for given Reynolds number, valid for, $0.3 \le t/e \le 0.5$, $0.3 \le t/p \le 0.5$, and $5 \cdot 10^4 \le \mathrm{Re} \le 1.5 \cdot 10^5$.

References

[1] Han, J. C., *et al*., Developing Heat Transfer in Rectangular Channels with Rib Turbulators, *International Journal of Heat & Mass Transfer*, *31* (1988), 1, pp. 183-195
[2] Hans, V. S., *et al*., Performance of Artificially Roughened Solar Air Heaters – A Review, *Renewable & Sustainable Energy Reviews*, *13* (2009), 8, pp. 1854-1869
[3] Han, J. C., Heat Transfer and Friction in Channels with Two Opposite Rib-Roughened Walls, *Journal of Heat Transfer*, *106* (1984), 4, pp. 774-781
[4] Kim, K. M., *et al*., Optimal Design of Angled Rib Turbulators in a Cooling Channel, *Heat & Mass Transfer*, *45* (2009), 12, pp. 1617-1625
[5] Alkhamis, N. Y., *et al*., Heat Transfer and Pressure Drop Correlations for Square Channels with V-Sshaped Ribs at High Reynolds Numbers, *Journal of Heat Transfer*, *133* (2011), 11, pp. 111901
[6] Lei, J., *et al*., Effect of Rib Spacing on Heat Transfer in a Two Pass Rectangular Channel (AR = 2:1) at High Rotation Numbers, *Asme Turbo Expo: Turbine Technical Conference & Exposition, 124* (2012), 9, 091901
[7] Sunden, B., Heat Transfer and Fluid Flow in Rib-Roughened Rectangular Ducts, in: *Heat Transfer Enhancement of Heat Exchangers,* (Eds. S. Kakaç, A. E. Bergles, F. Mayinger, H. Yüncü), Springer, Dordrecht, UK, 1999, pp. 123-140
[8] Maurer, M., *et al*., Experimental Study of Advanced Convective Cooling Techniques for Combustor Liners, *Proceedings,* Heat Transfer, Parts A and B, ASME Turbo Expo 2008: Power for Land, Sea, and Air, Berlin, Germany, 2008, Vol. 4, pp. 1779-1789

[9] Alfarawi, S., *et al*., Experimental Investigations of Heat Transfer Enhancement from Rectangular Duct Roughened by Hybrid Ribs, *International Journal of Thermal Sciences*, *118* (2017), Aug., pp. 123-138
[10] Liou, T. M., *et al*., Simulation and Measurement of Enhanced Turbulent Heat Transfer in a Channel with Periodic Ribs on One Principal Wall, *International Journal of Heat and Mass Transfer, 36* (1993), 2, pp. 507-517
[11] Bailey, J. C., *et al*., Heat Transfer and Friction in Channels with Very High Blockage 45° Staggered Turbulators, *Proceedings,* Turbo Expo 2003, Parts A and B, ASME Turbo Expo 2003, collocated with the 2003 International Joint Power Generation Conference, Atlanta, Geo., USA, 2003, 5, pp. 451-458
[12] Chanteloup, D., *et al*., Combined 3D Flow and Heat Transfer Measurements in a 2-Pass Internal Coolant Passage of Gas Turbine Airfoils, *Journal of Turbo machinery*, *124* (2002), 4, pp. 710-718
[13] Viswanathan, A. K., Tafti, D, K., Detached Eddy Simulation of Flow and Heat Transfer in Fully Developed Rotating Internal Cooling Channel with Normal Ribs, *International Journal of Heat & Fluid Flow*, *27* (2006), 3, pp. 351-370
[14] Carcasci, C., *et al*., Heat Transfer and Pressure Loss Measurements of Matrix Cooling Geometries for Gas Turbine Airfoils, *Journal of Turbomachinery*, *136* (2014), 12, pp. 121005
[15] Taslim, M. E., *et al*., Experimental Heat Transfer and Friction in Channels Roughened with Angled, V-shaped, and Discrete Ribs on Two Opposite Walls, *Journal of Turbomachinery*, *118* (1996), 1, V004T09A018
[16] Pandey, P. K., *et al*., A Finite Difference Method for a Numerical Solution of Elliptic Boundary Value Problems, *Applied Mathematics & Nonlinear Sciences*, *3* (2018), 1, pp. 311-320
[17] Alfonso, M. J. F. I., *et al*., Some Improvements on Relativistic Positioning Systems, *Applied Mathematics & Nonlinear Sciences*, *3* (2018), 1, pp. 161-166
[18] Luan, Y., *et al*., Numerical Investigation on Flow and Heat Transfer in Matrix Cooling Channels for Turbine Blades, *Proceedings*, Heat Transfer, ASME Turbo Expo 2016: *Turbomachinery Technical Conference and Exposition*, Seoul, South Korea, 2016, 5B, pp. V05BT11A005

Paper submitted: July 2, 2019
Paper revised: September 11, 2019
Paper accepted: September 19, 2019